CONTACT SENSOR PROCESSING FOR ACOUSTIC INSTRUMENT RECORDING USING A MODAL ARCHITECTURE

Mark Rau, Jonathan S. Abel, and Julius O. Smith III

Center for Computer Research in Music and Acoustics,
Stanford University
Stanford, USA
[mrau|abel|jos]@ccrma.stanford.edu

ABSTRACT

This paper proposes a method to filter the output of instrument contact sensors to approximate the response of a well placed microphone. A modal approach is proposed in which mode frequencies and damping ratios are fit to the frequency response of the contact sensor, and the mode gains are then determined for both the contact sensor and the microphone. The mode frequencies and damping ratios are presumed to be associated with the resonances of the instrument. Accordingly, the corresponding contact sensor and microphone mode gains will account for the instrument radiation. The ratios between the contact sensor and microphone gains are then used to create a parallel bank of second-order biquad filters to filter the contact sensor signal to estimate the microphone signal.

1. INTRODUCTION

Acoustic string instruments often lack the radiated sound power to compete with louder instruments such as drums or piano in a live or recording scenario. The most natural way to amplify their sound is using a well placed microphone, but this can be problematic as feedback and "bleed" sound from other instruments are common. To overcome these problems, pickups or contact sensors are used as they more directly capture the instrument's vibrations. Electromagnetic pickups are used with electric guitars, but they capture the strings' vibration and do not capture an authentic sound image of the instrument's body vibrations. Contact sensors such as piezoelectric or electret film sensors are more commonly used with acoustic instruments as they primarily capture the vibrations of the instrument, not purely of the strings.

In this paper, we focus on the upright bass as a test case. When used in a live jazz context, the upright bass almost always requires amplification. The most common method of achieving amplification is by using a contact sensor, typically piezoelectric, and routing the output to an amplifier. The resulting output bares little resemblance to the acoustic sound radiated by the instrument, and typically has a "rubbery" characteristic. In addition to the live scenario, it is often necessary to record upright bass in the same room as other instruments which are much louder, such as a piano or drum set. The sound of these instruments bleeds into the microphones meant for the upright bass, making it difficult to isolate the instrument or apply post-processing. It would be advantageous if the upright bass could be recorded using a contact sensor to achieve an isolated recording, but this is not often done as the acoustic response is desired.

Acoustic instrument contact sensors can be equalized, often in an attempt to make them sound more similar to the instrument's acoustically radiated sound. Commercially available acoustic instrument equalizers are limited in use and require trial and error to achieve a desirable sound. If an instrument's body is approximated as linear and time-invariant system, a transfer function between various point of measurement can be defined which will allow digital signal processing (DSP) techniques to force a signal captured at one location to sound more similar to a signal captured at a different location.

Such DSP equalization has been studied previously by Karjalainen et al. [1, 2, 3]. This work focused on the case of an acoustic guitar with an electret film pickup, and aimed to find a transfer function which was the spectral ratio of microphone and contact sensor transfer functions:

$$Q(\omega) = \frac{P(\omega)}{X(\omega)} , \tag{1}$$

where $Q(\omega)$ is an equalizer transfer function, $P(\omega)$ is the acoustic radiation transfer function measured with a microphone, and $X(\omega)$ is the transfer function through a contact sensor. They found transfer functions by first using an impact hammer to excite an impulse, and second by playing musical information through both sensors and deconvolving the contact sensor signal from the microphone signal. They constructed filters based on both of these methods using FIR and IIR structures. It was concluded that the deconvolution method paired with an FIR filter of order 500 or higher with an additional digital resonator tuned to the mode of the guitar's top plate produced the most desirable sound.

Rather than using a spectral ratio based approach, we propose a modal architecture which can be constructed where the mode frequencies and damping ratios are fit to the contact sensor frequency response, and the mode gains are taken as a ratio between the gains fit to the contact sensor and microphone frequency responses. A parallel bank of second-order biquad filters can be used to realize the filter in real time. A modal architecture is chosen because it is modular and has the potential to be altered in real time. This provides the option to choose from or mix between different microphone responses by tuning only the relative mode gains. This can be extended to the case of producing multiple simultaneous simulated microphone responses, which can be efficiently computed because the same set of mode filter outputs can be used to form each microphone's output according to its set of gains.

Much prior work has been done on modeling instrument transfer functions using a modal architecture [4, 5, 6, 7]. This work is typically done in the context of sound synthesis, but is equally valid for the proposed sensor equalization application. The mode parameters can be fit using traditional mode fitting techniques such as the Complex Exponential or Peak Picking methods [8, 9, 10]. The modal fits can be improved using a constrained optimization algorithm to reduce the error between the experimental and reconstructed frequency response functions [5, 11]. We follow an approach similar to these prior methods, calculating initial mode parameter guesses and using a constrained optimization to improve the reconstructed model.

This paper is organized as follows. Section 2 introduces the process for acquiring instrument impulse response data. Section 3 describes the modal parameter fitting and optimization, and Section 4 describes the steps needed to realize the model as a digital filter. Section 5 presents preliminary results, and Section 6 is a conclusion and discussion of potential improvements and further areas of study.

2. MEASUREMENTS

The proposed method relies on impulse response measurements which serve as the basis for a modal model. An upright bass was used as a case study for measurements and fitting. The upright bass was suspended from the ceiling with the endpin rested on foam for stability. Paper was woven between the strings to prevent them from ringing. An anechoic chamber was not available so the measurements were taken in a medium sized room with ample absorption.

Two commercially available contact sensors were attached to the bass for recording. A piezoelectric sensor was placed under the treble foot of the bridge, and a dynamic contact microphone was placed on the top plate, below the bridge. Five studio microphones were placed in various positions around the bass. The positions were chosen such that they may be typical starting positions for a studio recording of the upright bass. While multiple microphones and contact sensors were used to record the measurements, only one contact sensor and microphone pair is analyzed in this paper. The contact sensor and microphone placements can be seen in Figure 1, with the contact sensor and microphone pair of interest labeled.

A force sensing impact hammer was used to excite an impulse through the instrument. The hammer was struck on the bass side of the bridge, perpendicular to the curvature of the bridge at that location. The bass side of the bridge was chosen as the impact location because it is closest to the lowest string which provides the greatest amount of energy transfer. The hammer was remotely dropped multiple times, while the sensors and microphones recorded the impulse responses at their respective locations.

3. MODE FITTING

3.1. Modal Structure

Modal analysis can be used to investigate the vibrational characteristics of physical structures such as musical instruments [12]. The measured vibrational characteristics of a structure can be described by its frequency response function (FRF) which is a measurement function used to identify the resonant frequencies, damping ratios, and mode shapes of a physical structure. The frequency response function between points p and q of a modal structure can be written as

$$H_{pq}(s) = \sum_{r=1}^{N} \frac{\psi_{pr}\psi_{qr}}{(s^2 + 2\Omega_r\zeta_r s + \Omega_r^2)}\ , \tag{2}$$

where r is the mode number up to a maximum number of modes, N. The undamped natural frequency Ω_r is defined as $\Omega_r = \sqrt{\sigma_r^2 + \omega_r^2}$, where σ_r is the damping factor and ω_r is the damped natural frequency. The damping ratio ζ_r is defined as $\zeta_r = -\frac{\sigma_r}{\Omega_r}$. The mode shape coefficients at points p and q are ψ_{pr} and ψ_{qr} [13].

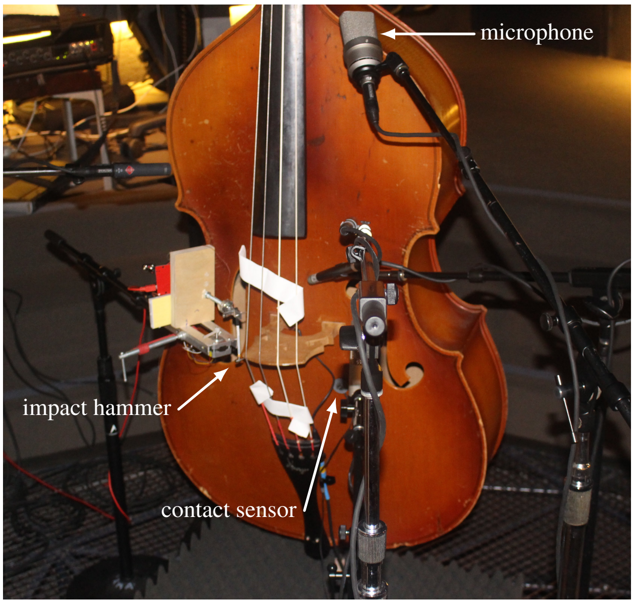

Figure 1: *Measurement setup.*

3.2. Measurement Preprocessing

Due to the non-anechoic nature of the room and the low amount of energy transferred to the instrument from the impact hammer, the impulse response measurements required preprocessing to allow reliable transfer function fits.

Roughly 100 impulse measurements were taken. Measurements containing double hits from the hammer were discarded. Each impulse was windowed using an exponential window to improve the signal-to-noise ratio [14]. Frequency response functions were calculated for each pair of hammer excitation and sensor signals. The frequency response function is calculated for each measurement set using Welch's method and they are averaged in the frequency domain to reduce random error [13].

3.3. Initial Mode Fitting

An initial pass is made on the mode fitting which uses the Complex Exponential method [9]. The Complex Exponential method computes the time domain impulse response corresponding to the given frequency response function, and a set of complex damped sinusoids is fit using Prony's method. This is a nonlinear process which finds a solution iteratively.

The initial mode fitting process is performed over 9 different frequency bands ranging from 0 to 6 kHz, and the number of modes to fit was determined by eye. The Complex Exponential mode fitting returns estimates of Ω_r, $\hat{\zeta}_r$, and Ψ_r, the product of the complex mode shapes at the impact and measurement locations. The damping ratios $\hat{\zeta}_r$ represent damping ratios fit to the windowed impulse response measurements. Since an exponential decay window is used, it introduces additional damping which will be corrected for at a later point. The returned undamped natural frequencies and damping coefficients were reasonably fit, but the mode shapes were not as reliable so they were recomputed using the least squares method.

3.4. Choice of Modes

The frequency response function was computed for each sensor location, yielding multiple sets of mode parameters. Theoretically, each set of mode parameters should contain the same undamped natural frequencies, and damping coefficients, varying only by mode shape. However, if a measurement sensor is at or near a relative node location, it is unlikely that an undamped natural frequency will be fit to the frequency response function. Likewise, if a mode is present at a sensor location, it still may be missed due to the measurement noise or the windowing process. Even if a mode is present in multiple sensor measurements, there will likely be numerical differences between mode fittings.

A method was developed to create a set of mode parameters which is common between multiple frequency response functions. A set of common mode parameters is created based on common undamped natural frequencies, worrying about the damping ratios at a later point. Let S_C be a set of undamped natural frequencies measured through a contact sensor, and let $S_{M_1}, ..., S_{M_N}$ be sets of undamped natural frequencies measured through N microphones at various locations around the instrument. To get the set of all undamped natural frequencies present, a union of sorts is taken.

To account for numerical differences between undamped natural frequencies that are common between both sensor sets, a tolerance δ is set, within which there is deemed to be only one unique mode. The undamped natural frequencies in S_C are taken as the true undamped natural frequencies, as only direct measurements from the contact sensor will be used in the final processing. The modes from S_{M_i} which have undamped natural frequencies within δ percent of the undamped natural frequencies in S_C are discarded. This can be summarized as

$$\hat{S}_{M_i} = S_{M_i} \setminus ((1 \pm \delta) S_C) \ , \tag{3}$$

where $\setminus$ represents the set difference, and $\hat{S}_{M_i}$ is the set of undamped natural frequencies only present in S_{M_i} within the set tolerance δ. The set of undamped natural frequencies found in all sensors of interest can then be represented as

$$S_F = S_C \cup \left(\hat{S}_{M_1} \cup ... \cup \hat{S}_{M_N}\right) \ , \tag{4}$$

where $\cup$ represents the set union.

The initial guesses for the damping ratios and mode shapes correspond to the undamped natural frequencies in S_F.

This method for choosing the mode shapes is general to any number of microphone frequency response functions, but for the rest of the paper, a setup consisting of one contact sensor and one microphone is assumed.

3.5. Optimized Mode Fitting

To further refine the modal fitting, a constrained optimization scheme is formed to minimize the error between the measured and reconstructed frequency response function pairs. The optimization problem is posed as

$$\underset{\Omega_r,\, \hat{\zeta}_r,\, \Psi_r}{\text{minimize}} \quad \varepsilon(\hat{H}_C,\, H_C,\, \hat{H}_M,\, H_M) \, , \tag{5}$$

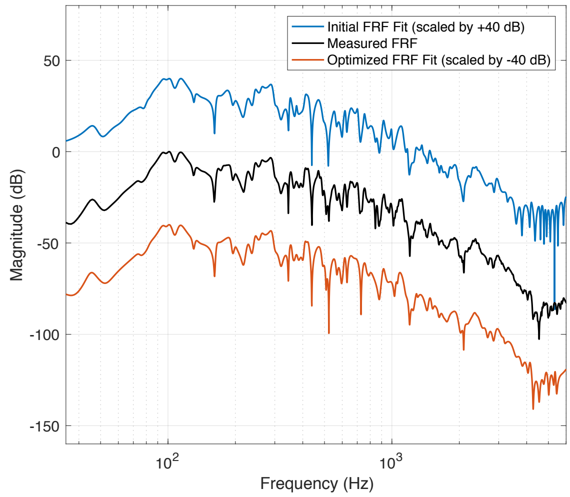

Figure 2: *Contact sensor frequency response function (FRF) and fits with $N = 88$ modes.*

where H_C and $\hat{H}_C$ are the measured and reconstructed frequency response functions for the contact sensor, H_M and $\hat{H}_M$ are the measured and reconstructed frequency response functions for the microphone, and $\varepsilon(\hat{H}_C, H_C, \hat{H}_M, H_M)$ is an error measure to be minimized. The initial mode fits calculated using the Complex Exponentials method are used as initial guesses for the optimization. The optimization constrains the values of Ω_r and $\hat{\zeta}_r$ to be within $\pm$ 50 % of the initial guess values.

During each iteration of the optimization, there is a guess for the values of Ω_r and $\hat{\zeta}_r$. These parameters are held constant for both contact sensor and microphone frequency response function reconstructions. Least squares is used to calculate the mode shapes Ψ_r^C and Ψ_r^M for the contact sensor and microphone modes respectively. The frequency response functions are reconstructed and the following error function is used:

$$\varepsilon(\hat{H}_C,\, H_C,\, \hat{H}_M,\, H_M) = ||H_C - \hat{H}_C||_1 + ||H_M - \hat{H}_M||_1 \ , \tag{6}$$

where $\hat{H}_C$ and $\hat{H}_M$ are the reconstructed frequency response functions using the same sets of undamped natural frequencies Ω_r and damping ratios $\hat{\zeta}_r$, but with their own sets of mode shapes Ψ_r^C and Ψ_r^M, and $|| \cdot ||_1$ is the L1-norm.

Example frequency response functions are shown for a dynamic contact sensor (Figure 2) and a cardioid studio microphone placed roughly 30 cm away from the the instruments top plate near the upper bout (Figure 3). The window exponential decay constant was set to $\beta = 0.07\ s^{-1}$, and the natural frequency tolerance was set to $\delta = 2$ %. The examples show the measured frequency response function as well as the frequency response functions recreated from the initial and optimized mode fits.

4. REALIZATION AS PARALLEL BANK OF SECOND-ORDER BIQUAD FILTERS

The goal of this study is to scale the contact sensor response such that it will better approximate that of the microphone. A choice was made to perform the mode fitting in the continuous domain to

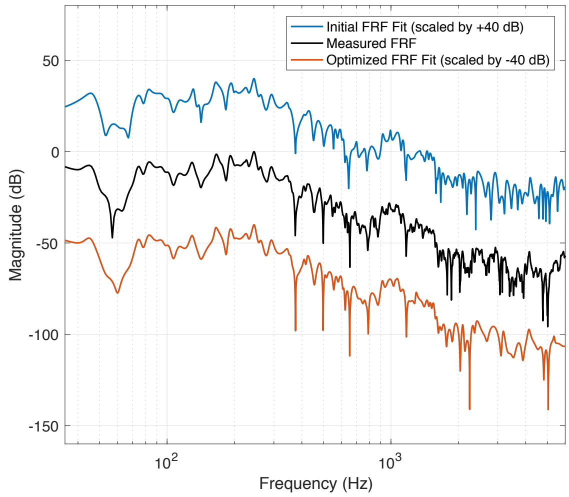

Figure 3: *Microphone frequency response function (FRF) and fits with* $N = 88$ *modes.*

maintain the physical parametric structure, and to later convert to the discrete domain to facilitate the DSP equalization. This equalization can be realized by using the obtained modal parameters to create a parallel bank of second-order biquad filters which can be described by their undamped natural frequencies, damping coefficients, and mode shapes or gains. The undamped natural frequencies Ω_r obtained using the previously described method can be used, but the damping ratios $\hat{\zeta}_r$ and mode shapes Ψ_r^C and Ψ_r^M need to be adjusted.

4.1. Mode Shape Scaling

It is assumed that the microphone and contact sensor measurements will contain the same set of undamped natural frequencies and damping coefficients, and will differ only by their relative mode shapes. In order to impose the microphone response on the contact sensor, a scaling needs to be performed between the mode shapes. This can be obtained by taking the ratio of the mode shapes

$$G_r = \frac{\Psi_r^M}{\Psi_r^C} , \tag{7}$$

which gives the scaling gain between the mode shapes G_r.

4.2. Damping Ratio Correction

The use of the exponential decay window adds additional damping to the measured frequency response which needs to be compensated for when creating the modal scaling filter. The exponential decay window is defined as

$$w_e(t) = e^{-\beta t} , \tag{8}$$

where β is the exponential decay constant. Figure 4 shows how the additional damping caused by the window results in a windowed damping ratio $\hat{\sigma}_r$, which is more negative than the true damping ratio σ_r, by the amount of the exponential decay constant used for the window, β.

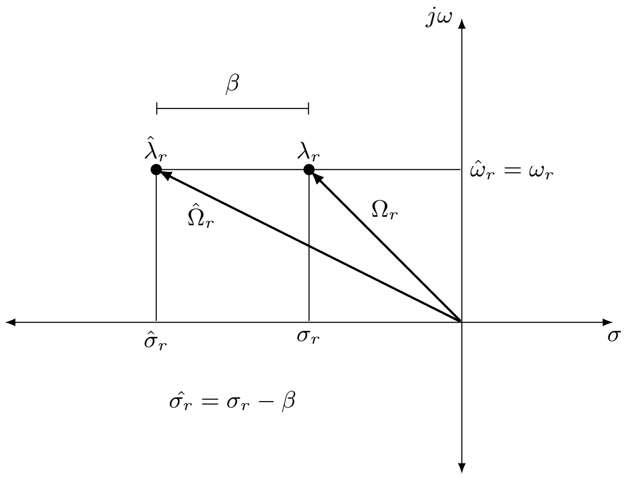

Figure 4: *Effect of the exponential decay window in the complex plane.* β *is the exponential decay constant of the window.* λ_r, ω_r, σ_r, *and* Ω_r *are the eigenvalue, damped natural frequency, damping factor, and undamped natural frequency for mode r.* $\hat{\lambda}_r$, $\hat{\omega}_r$, $\hat{\sigma}_r$, *and* $\hat{\Omega}_r$ *have the same meaning except for the windowed signal.*

A common correction approximation for the extra damping caused by the exponential decay window is given by

$$\zeta_r' = \hat{\zeta}_r - \frac{\beta}{\hat{\Omega}_r} , \tag{9}$$

where ζ_r' is an approximation to the true damping ratio $\hat{\zeta}_r$ is the damping ratio after the windowing effects, and $\hat{\Omega}_r$ is the undamped natural frequency of the windowed data [14]. The exact expression for the true damping ratio ζ_r is given in the Appendix.

4.3. Analog to Digital: Bilinear Transform

Substituting the corrected damping ratios ζ_r, and the gain between mode shapes G_r into (2) gives

$$Q(s) = \sum_{r=1}^{N} \frac{G_r}{(s^2 + 2\Omega_r \zeta_r s + \Omega_r^2)} , \tag{10}$$

which is the transfer function for the s-domain filter needed to scale the contact sensor.

The s-domain transfer function is converted to the discrete domain using the bilinear transform:

$$s = c_r \left(\frac{1 - z^{-1}}{1 + z^{-1}} \right) . \tag{11}$$

The natural frequencies are kept constant under the frequency warping caused by the bilinear transform by setting

$$c_r = \frac{\Omega_r}{\tan\left(\frac{\Omega_r}{2 f_s}\right)} , \tag{12}$$

where f_s is the sample rate.

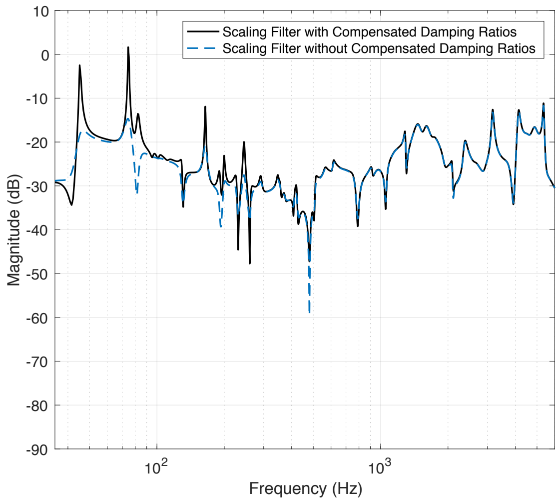

Figure 5: *Modal scaling filter frequency response with* $N = 85$ *modes.*

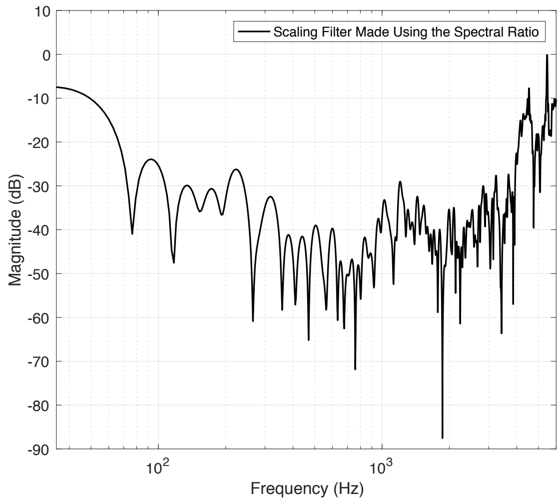

Figure 6: *Spectral ratio scaling filter frequency response implemented using a 1200 tap FIR filter.*

The resulting discrete transfer function is given by

$$Q_r(z) = \frac{b_0 + b_2 z^{-2}}{1 + a_1 z^{-1} + a_2 z^{-2}} \tag{13}$$

where

$$\begin{aligned} b_0 = b_2 &= \frac{G_r}{\Omega_r^2 + c_r^2 + 2c_r\Omega_r\zeta_r} \\ a_1 &= \frac{2\Omega_r^2 - 2c_r^2}{\Omega_r^2 + c_r^2 + 2c_r\Omega_r\zeta_r} \\ a_2 &= \frac{\Omega_r^2 + c_r^2 - 2c_r\Omega_r\zeta_r}{\Omega_r^2 + c_r^2 + 2c_r\Omega_r\zeta_r} . \end{aligned}$$

The modal scaling filter frequency response corresponding to the contact sensor and microphone from Figures 2 and 3 is shown in Figure 5. The frequency response is shown with and without the damping ratio correction.

5. RESULTS AND DISCUSSION

The modal architecture yields a parallel bank of second-order biquad filters which can be used to filter the output of an instrument through a contact sensor, resulting in a signal which should sound similar to that measured through a microphone.

As a comparison to the modal scaling filter, Figure 6 shows the equalization filter using the spectral ratio method of Karjalainen et al., for a 1200 tap FIR filter. The two filters are difficult to compare due to the low spectral resolution of the FIR filter, but some general comparisons can be made. Both filters exhibit a similar overall contour, having a higher magnitude in the low and high frequencies, with a lower magnitude in the mid frequency range of roughly 300-1000 Hz. However, while the general contours of the modal and spectral ratio equalization filters are similar, there are clear differences. Since the spectral ratio filter is implemented as a relatively short FIR filter, there is a low amount of mode resolution, making it impossible to accurately model resonant modes with low damping ratios. While the modal model is able to accurately capture highly resonant modes, it may be incorrectly modeling some modes resulting in discrepancies between the filters.

Figure 7 shows spectrograms of a hammer impulse measured through a contact sensor, a microphone, as well as the contact sensor signal filtered with the modal model. Figure 8 shows the output of the measured upright bass being played. The contact sensor, microphone, and filtered contact microphone sensor signals are shown. Audio examples of the filtered upright bass being played can be found online[1]. Qualitative observations suggest that the contact sensor filtered with the modal architecture is more acoustic sounding and similar to the microphone signal. The filtered contact sensor signal and microphone signal do not sound exactly the same, but this is to be expected as the sensor is only picking up the vibrations present at its location, so it cannot be expected to contain information about the other sounds produced by the instrument or performer.

The proposed modal architecture poses several advantages over the spectral ratio method of Karjalainen et al.. The mode gains can be altered in real time, allowing for on-line tuning of the equalization. This could be used to adjust individual modes which are problematic in a particular playing situation, say if a mode of the instrument is at the same frequency as a room mode of the performance space. If multiple microphone frequency response functions were modeled, this structure allows for simple switching between or interpolating between microphone responses. The major drawback of the modal architecture is the sensitivity of the mode parameter fitting.

The modal fitting is sensitive to the window's exponential decay constant, the set frequency tolerance, as well as the number of modes to be fit. As the window's exponential decay constant is decreased, the signal-to-noise ratio is improved, but the risk of missing modes in the fitting is increased. While decreasing the undamped natural frequency tolerance, the chance of fitting the same mode twice is minimized, but the chance of missing closely spaced modes is increased. Hence, the number of modes to fit is related to the window's exponential decay constant as well as the undamped

[1] https://ccrma.stanford.edu/~mrau/DAFX2018/

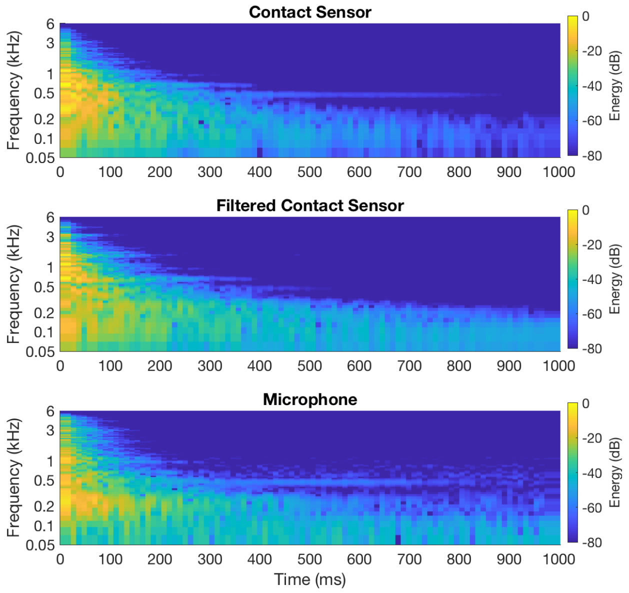

Figure 7: *Spectrogram of an impulse recording.*

natural frequency tolerance. Some trial and error is required to obtain the desired results.

The resulting filtered contact sensor sounds more acoustic, and similar to the the microphone signal; however, it is not perfect. There are likely multiple factors contributing to the differences. The measurements have a low signal-to-noise ratio and were recorded in a non-ideal location making the mode fitting challenging and sensitive to the windowing and parameter initialization. Notably, not all sounds present in the microphone signal will appear in the contact sensor signal. The contact sensor could be placed at a vibrational node of the instrument and will predominantly pick up vibrations in one direction. In this case, using multiple well placed contact sensors would overcome the problem. As well, any sounds such as finger motions on the strings are unlikely to be picked up by the contact sensor. Since these vibrations do not appear in the contact sensor signal, it will not be possible to recreate their presence in the microphone signal by filtering the contact sensor alone.

6. CONCLUSIONS

A modal analysis is developed to design filters to make instrument contact sensors sound more like microphones. An upright bass was used as a case study and impulse response measurements of the instrument were recorded through multiple contact sensors and microphones. The modal parameters are initially fit using the Complex Exponentials method, and are then improved upon using a constrained optimization scheme. The modal parameters are used to form a parallel bank of second-order biquad filters which can be used to equalize a contact sensor signal such that it sounds more similar to a microphone at a specific location.

Avenues for future study include further optimizing the modal architecture as well as expanding to and testing with multiple sensors at various locations. If multiple contact sensors are used, the chance that all sensors will be located at vibrational nodes is small, so there can be more confidence that all modes will be captured. If multiple microphones are used, the ability to interpolate between them to achieve a desirable microphone placement for the output signal is gained.

7. REFERENCES

[1] M. Karjalainen, V. Välimäki, H. Penttinen, and H. Saastamoinen, “DSP equalization of electret film pickup for the acoustic guitar,” *Journal of the Audio Engineering Society*, vol. 48, no. 12, pp. 1183–1193, 2000.

[2] M. Karjalainen, H. Penttinen, and V. Välimäki, “Acoustic sound from the electric guitar using DSP techniques,” in *Acoustics, Speech, and Signal Processing, 2000. ICASSP’00. Proceedings. 2000 IEEE International Conference on*. IEEE, 2000, vol. 2, pp. II773–II776.

[3] M. Karjalainen, H. Penttinen, and V. Välimäki, “More acoustic sounding timbre from guitar pickups,” *in 2nd Workshop on Digital Audio Effects (DAFx-99), Trondheim, Norway*, vol. 10, pp. 1–4, Dec. 9–11, 1999.

[4] M. Karjalainen and J. O. Smith, “Body modeling techniques for string instrument synthesis,” in *International Computer Music Conference (ICMC)*, 1996, pp. 232–239.

[5] E. Maestre, G. P. Scavone, and J. O. Smith, “Digital modeling of bridge driving-point admittances from measurements on violin-family instruments,” in *Proc. of the Stockholm Music Acoustics Conference*, 2013, pp. 101–108.

[6] E. Maestre, G. P. Scavone, and J. O. Smith, “Digital modeling of string instrument bridge reflectance and body radiativity for sound synthesis by digital waveguides,” in *Applications of Signal Processing to Audio and Acoustics (WASPAA), 2015 IEEE Workshop on*. IEEE, 2015, pp. 1–5.

[7] J. O. Smith, *Physical Audio Signal Processing*, W3K Publishing, 2004, online book: `http://ccrma.stanford.edu/~jos/pasp/`.

[8] P. Antsalo, A. Mäkivirta, V. Välimäki, T. Peltonen, and M. Karjalainen, “Estimation of modal decay parameters from noisy response measurements,” in *Proc. Audio Eng. Soc. (AES) Conv., Amsterdam, The Netherlands*, May 12–15, 2001, vol. 110, pp. 867–878.

[9] D. Brown, R. Allemang, R. Zimmerman, and M. Mergeay, “Parameter estimation techniques for modal analysis,” Tech. Rep., SAE Technical paper, 1979.

[10] D. Ewins, *Modal Testing: Theory and Practice*, vol. 15, Research studies press Letchworth, 1984.

[11] E. Maestre, J. S. Abel, J. O. Smith, and G. P. Scavone, “Constrained pole optimization for modal reverberation,” *in 20th Int. Conf. Digital Audio Effects (DAFx-17), Edinburgh, UK*, pp. 381–388, Sep. 5–9, 2017.

[12] N. Fletcher and T. Rossing, *The Physics of Musical Instruments*, Springer-Verlag, 1991.

[13] A. Brandt, *Noise and Vibration Analysis: Signal Analysis and Experimental Procedures*, John Wiley & Sons, 2011.

[14] W. Fladung and R. Rost, “Application and correction of the exponential window for frequency response functions,” *Mechanical systems and signal processing*, vol. 11, no. 1, pp. 23–36, 1997.

[15] H. Penttinen and M. Tikander, "Sound quality differences between electret film (EMFIT) and piezoelectric under-saddle guitar pickups," in *Proc. Audio Eng. Soc. (AES) Conv., Paris, France*, May 20–23, 2006, vol. 120.

[16] B. Peeters, J. Lau, J. Lanslot, and H. Van der Auweraer, "Automatic modal analysis-Myth or reality?," *Sound and Vibration*, vol. 42, no. 3, pp. 17–21, 2008.

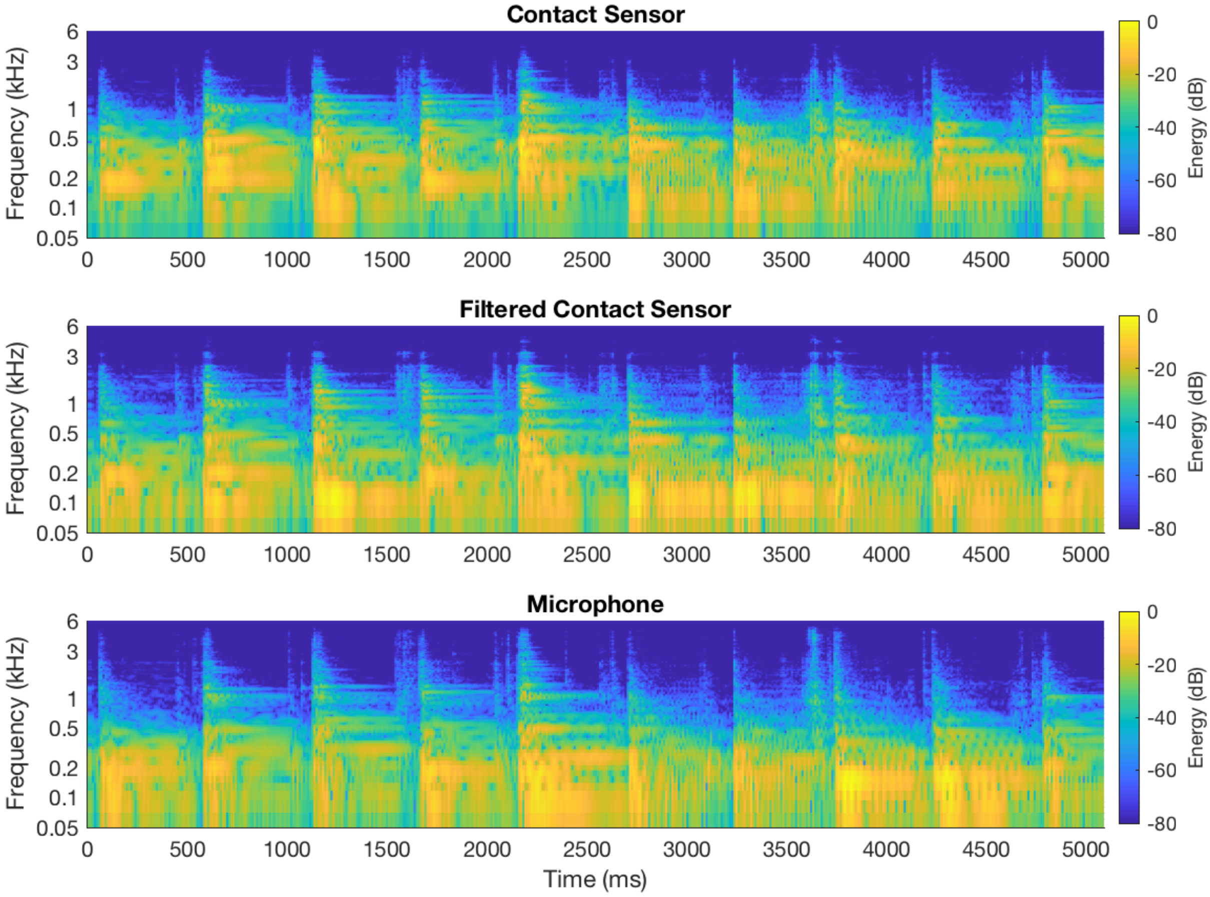

Figure 8: *Spectrogram of the bass being played.*

APPENDIX: DAMPING RATIO COMPENSATION

The exact representation of the original damping coefficient before windowing using the exponential decay window can be found by solving the equation:

$$\zeta_r = \frac{\sqrt{1-\zeta_r^2}}{\sqrt{1-\hat{\zeta}_r^2}}\hat{\zeta}_r - \frac{\beta\sqrt{1-\zeta_r^2}}{\omega_r}, \tag{14}$$

which yields the two solutions:

$$\zeta_r \to \pm\frac{\sqrt{\beta^4\hat{\zeta}_r^{\,4} - 2\beta^4\hat{\zeta}_r^{\,2} + \beta^4 + 3\beta^2\omega_r^2\hat{\zeta}_r^{\,4} - 4\beta^2\omega_r^2\hat{\zeta}_r^{\,2} + \beta^2\omega_r^2 - 2\beta\omega_r^3\hat{\zeta}_r\sqrt{1-\hat{\zeta}_r^{\,2}} + 2\beta\omega_r^3\hat{\zeta}_r^{\,3}\sqrt{1-\hat{\zeta}_r^{\,2}} + \omega_r^4\hat{\zeta}_r^{\,2}}}{\sqrt{\beta^4\hat{\zeta}_r^{\,4} - 2\beta^4\hat{\zeta}_r^{\,2} + \beta^4 + 4\beta^2\omega_r^2\hat{\zeta}_r^{\,4} - 6\beta^2\omega_r^2\hat{\zeta}_r^{\,2} + 2\beta^2\omega_r^2 + \omega_r^4}}. \tag{15}$$

Two solutions are found, but the damping ratio must be positive for a damped system, so the positive solution must be used.